**Article**

# Discovery of potent inhibitors of *Schistosoma mansoni* NAD catabolizing enzyme

Sylvain A. Jacques, Isabelle Kuhn, Oleksandr Koniev, Francis Schuber, Frances E. Lund, Alain Wagner, Hélène Muller-Steffner, and Esther Kellenberger

## Just Accepted

# Discovery of potent inhibitors of *Schistosoma mansoni* NAD⁺ catabolizing enzyme

*Sylvain A. Jacques[1,2], Isabelle Kuhn[1], Oleksandr Koniev[1], Francis Schuber[1], Frances E. Lund[3], Alain Wagner[1], Hélène Muller-Steffner*[1] and Esther Kellenberger*[2]*

[1] Laboratoire des Systèmes Chimiques Fonctionnels, CAMB UMR7199 CNRS/ Université de Strasbourg, MEDALIS Drug Discovery Center, Faculté de Pharmacie, 67401 Illkirch, France

[2] Laboratoire d'Innovation Thérapeutique, LIT UMR7200 CNRS/Université de Strasbourg, MEDALIS Drug Discovery Center, Faculté de Pharmacie, 67401 Illkirch, France

[3] Department of Microbiology, University of Alabama at Birmingham, 276 BBRB Box 11, 1720 2nd Avenue South, Birmingham AL, United States of America

ABSTRACT. The blood fluke *Schistosoma mansoni* is the causative agent of the intestinal form of schistosomiasis (or bilharzia). Emergence of *Schistosoma mansoni* with reduced sensitivity to praziquantel, the drug currently used to treat this neglected disease, has underlined the need for development of new strategies to control schistosomiasis. Our ability to screen drug libraries for anti-schistosomal compounds has been hampered by the lack of validated *S. mansoni* targets. In the present work, we describe a virtual screening approach to identify inhibitors of *S. mansoni* $NAD^+$ catabolizing enzyme (*Sm*NACE), a receptor enzyme suspected to be involved in immune evasion by the parasite at the adult stage. Docking of commercial libraries into a homology model of the enzyme has led to the discovery of two *in vitro* micromolar inhibitors. Further structure-activity relationship studies have allowed a 3-log gain in potency, accompanied by a largely enhanced selectivity for the parasitic enzyme over the human homolog CD38.

INTRODUCTION

Schistosomiasis is a chronic neglected tropical disease. It affects over 200 million people and is more debilitating than malaria.[1, 2] It is caused by helminth parasites of the genus Schistosoma. The mostly studied species is *Schistosoma mansoni*, which causes the intestinal form of the disease. *S. mansoni* adult worms live in the portal vasculature and produce eggs, which damage liver and intestinal tissues. The long-term survival of the parasite in the host involves a remarkable control of the host immune system, in particular through an appropriately balanced T helper response.[3, 4] Molecular mechanisms of this immune-evasion are far from being unraveled. A better understanding of the host-parasite relationship is needed to facilitate vaccine design[5] and to identify new drugs effective against the adult worms, especially those with reduced sensitivity to the prevalent antischistosomal drug praziquantel.[6]

In 2005, we identified a novel enzyme, *S. mansoni* NAD$^+$ catabolizing enzyme (*Sm*NACE), which is expressed on the outer surface of the *S. mansoni* adult worm tegument.[7] This enzyme is a distant homolog of the mammalian CD38, a membrane-associated ecto-enzyme which has the potential to regulate innate and adaptive immune responses.[8] Like CD38, *Sm*NACE is an efficient NAD$^+$ glycohydrolase. However it lacks the cADPR cyclase activity which is the hallmark of CD38.[9] In human, cADPR produced by CD38 is a calcium-mobilizing metabolite involved in the chemotactic response of human neutrophils and monocytes to inflammatory chemokines.[8] Accordingly, it is tempting to postulate that *Sm*NACE acts as an "immune evasion" molecule for *S. mansoni* by decreasing substrate availability for CD38 and preventing the CD38 expressing host cells from producing cADPR.

To better characterize *Sm*NACE function, and eventually validate its potential as a pharmacological target for antischistosomal therapy, we set out to identify inhibitors of its enzymatic activity. We recently screened a subset of the French National Library (13 760

molecules) and the Prestwick Chemical Library (880 drugs), and identified two micromolar

inhibitors, cyanidin and delphidin.[10] However, these two molecules are poor chemical tools

for studying the *in vivo* function of *Sm*NACE, due to a general lack of selectivity that is

characteristic of the anthocyanidin family of natural products to which they belong.

In the present study, the virtual screening of commercial libraries (*ca.* 2 million of

molecules) by high-throughput docking into a *Sm*NACE homology model allowed the

identification of a competitive inhibitor (numbered **3a** in Scheme 1) of the enzyme. We report

the synthesis of analogs of **3a** and their inhibitory effect on *Sm*NACE catalytic function *in*

*vitro*. Furthermore, we show that the best inhibitors in the series have nanomolar potency and

are selective for *Sm*NACE *versus* the human homolog CD38.

RESULTS AND DISCUSSION

**Virtual screening.** The 3D structure of *Sm*NACE was modeled by homology to human and

bovine CD38, *Aplysia* cyclase and human BST1. Because of the low sequence identity

between *Sm*NACE and the template proteins (from 19.7% to 23.7%), the multiple alignment

was guided by structural data, especially disulfide bridges and conserved secondary

structures. The active site was particularly well defined because it was mainly composed of

conserved secondary structure elements.[9]

The *Sm*NACE model was used to virtually screen a non-redundant selection of commercial

compounds by high-throughput docking (Figure 1). An initial filtering biased the dataset

towards compounds of small molecular weight in agreement with the small size of the active

site of *Sm*NACE. The molecular weight distribution fitted a Gaussian function centered on

310 with a medium height width of 175. More than 60 000 molecules were docked into the

target. About 3% of the docking poses passed the scoring filters. In 6.9% of these selected

poses, the predicted inter-molecular interactions partly matched that observed in at least one crystal structure of CD38 in complex with a substrate, products or molecular analogs (Tanimoto coefficient computed on interaction fingerprints greater than 0.6). Additional 1.4% of poses were retained based on interaction fingerprints, using a machine learning approach trained to discriminate inter-molecular interactions in crystal structures of CD38 in complex with a substrate, products or molecular analogs from "decoy" binding modes generated by the docking into *Sm*NACE of truly inactive compounds. The automated selection protocol returned 188 molecules. A visual inspection rejected 90 molecules because of high similarity between structures.

**Biological validation of hits.** The 98 selected compounds were purchased and tested for their ability to inhibit the catalytic activity of recombinant *Sm*NACE *in vitro* using 1,N[6]-etheno NAD^{+} as substrate. In the case of molecules with intrinsic fluorescence, the inhibition of *Sm*NACE was re-evaluated using the direct quantification by HPLC of the reaction products generated using NAD^{+} as substrate. We observed that 20 molecules produce a significant inhibition ($\geq$ 10%) at a concentration of 100 µM. We further tested the preliminary hits by repeating both fluorimetric and HPLC assays at different inhibitor concentrations. Only five molecules consistently inhibited more than 40% of *Sm*NACE activity at a concentration of 100 µM. One of these molecules was taxifolin, which was already investigated as *Sm*NACE inhibitor because of its similarity to cyanidin.[10] As mentioned in the Introduction, cyanidin and taxifolin are natural products with multiple biological activities due to promiscuous binding to different protein targets. We therefore focused our study on the other four molecules. We repeated the *in vitro* enzymatic experiments on four new lots of chemicals (purchased from a different supplier or synthesized if not available commercially), as well as on two or three close chemical analogs of each of the four molecules. Three out of the four putative inhibitors have been discarded

because the investigated changes in the structure (e.g., loss of a carboxyl group) had dramatic effects on the inhibitory effect, or because inhibition was not reproducible due to fluorescence quenching and/or compound degradation. In the end, only one of the four potential inhibitors has been validated (Figure 2a). The construction of the dose response curve revealed a half maximal inhibition concentration ($IC_{50}$) equal to $88 \pm 8$ µM (Figure 2b). Though the inhibition potency is modest, it nevertheless corresponds to a fairly good ligand efficiency (0.30 kcal/mol/heavy atom)[11] because the molecular mass of the inhibitor is small (260.25 Da). For the sake of comparison, we observed exactly the same ligand efficiency for the racemic form of taxifolin ($IC_{50}$: $19.5 \pm 1.4$ µM).[10] Lastly, Dixon plots unambiguously established that, like taxifolin, the validated hit is a competitive inhibitor of *Sm*NACE (Figure 2c). The docking poses of taxifolin and of the validated inhibitor are given as Supplementary Material (Figure S1).

**Chemistry.** The synthetic route of the target modified hydrazide derivatives obtained by condensation reactions is outlined on Scheme 1. Commercially available methyl 2-methylfuran-3-carboxylate (**1**) was converted into the corresponding hydrazide **2** using hydrazine monohydrate,[12] and the hydrazide was reacted with substituted aldehydes or ketones to give the corresponding compounds **3a–3p**.[13] Benzylidene-carbohydrazide derivatives **3d** and **3e** were treated with TFA and triethylsilane to afford compounds **4b** and **4c**.[14] Treatment of **3e** with methyl iodide gave compound **8**. Saponification of **1** with NaOH [15] followed by activation of the acid with ethyl chloroformate and condensation with 2-(2-methoxyphenyl)ethan-1-amine gave amide **6** (Scheme 2). Finally compounds **6** and **8** were converted into the corresponding phenols **5** and **7**, respectively upon treatment with $BBr_3$ at low temperature. Bis-amide derivatives **11a**-**11d** were obtained by acylation reactions between acid chloride and hydrazide derivatives (Scheme 3). Carboxylic acid **9** was

converted into the corresponding acid chloride by treatment with oxalyl chloride and DMF and reacted with commercially available hydrazide **10** to give **11a**. [16] In a similar manner, compounds **11b**-**11d** were prepared by reacting hydrazide **2** with the corresponding acid chlorides derived from commercially available or easily prepared carboxylic acids **13b**-**13d**. Finally, 1,3,4-oxadiazole derivatives **12a**–**12c** were obtained upon treatment of **11a**-**11c** with dehydrating reagent 2-chloro-1,3-dimethylimidazolinium chloride (DMC) in the presence of $Et_3N$.[17]

**Structure-Activity Relationships.** We have assessed the importance of the two hydroxyl groups in the validated hit (**3a**). To that end we compared the effect on *Sm*NACE inhibition *in vitro* of five different substitution patterns of the phenyl ring (Table 1, compounds **3b**-**3e**, **3o**). Methylation of the meta hydroxyl group (**3b**) did not affect the $IC_{50}$ value. By contrast, a 4-fold decrease of the apparent affinity was observed for the fully dehydroxylated analog (**3c**, with $IC_{50}$=330μM). Single substitution at position 1 (**3d**, with $IC_{50}$=0.13μM) resulted in a 3-log gain in affinity as compared to **3a**. Considering **3d**, the introduction of a methoxy group at position 1 (**3e**, with $IC_{50}$=67μM) or of a second hydroxyl group at position 2 (**3o**, with $IC_{50}$=8.7μM) was detrimental to the activity.

Starting from the best inhibitor **3d**, we tested other substitutions at positions 2-4 of the phenyl ring (Table 1, compounds **3f**-**3n**). Considering position 2, substitution with fluorine (**3h**, with $IC_{50}$=0.036μM) resulted in a 4-fold improvement of $IC_{50}$ as compared to **3d**, whereas substitution with chlorine (**3f**, with $IC_{50}$=0.15μM) did not significantly modify the $IC_{50}$ value, and introduction of an alkyl group (**3m** and **3n**, with respectively $IC_{50}$=59μM and $IC_{50}$=105μM) negatively impacted inhibitory potency. Introduction of chlorine or methoxy group(s) at positions 3 (**3k**), 4 (**3g** and **3j**) and 3,5 (**3i**) also decreased $IC_{50}$ values (1.5 to 4 fold, $IC_{50}$=0.032-0.077μM). This round of modification allowed a significant improvement of ligand efficiency, which reached 0.54 kcal/mol/heavy atom for **3g** and **3h**.

We then investigated whether the nature of the linker between the phenyl and furan rings impacts activity on *Sm*NACE. Increasing the linker flexibility in **3d** by reduction of the C=N double bond (**4b**) or its replacement by C-C single bond (**5**) dramatically increased $IC_{50}$ values ($IC_{50}$=12.3µM and $IC_{50}$=131µM, respectively). The same modifications made on the *O*-methylated inhibitor **3e** (**4c, 6**) also decreased the inhibitor potency ($IC_{50}$=11.6µM and 0% inhibition at 100µM concentration, respectively). The introduction of a methyl group on the amide nitrogen atom of **3e** (**8**) also produced a substantial drop of inhibition ($IC_{50}$=513µM), suggesting that the hydrogen atom of the amide may be involved in an important intramolecular or intermolecular H-bond. We further modified the H-bonding properties of three compounds with the introduction of a bis-amide linker, yet no significant changes in activity were observed (**11a**–**11c** *vs* parent compounds **3d**, **3g** and **3k**). Lastly, a rigid 1,2,4-oxadiazole linker completely abolished the ability to inhibit *Sm*NACE (**12a**– **12c**, with 0% inhibition at 100µM concentration).

Overall, the study of structure-activity relationships has identified eleven potent inhibitors of *Sm*NACE with $IC_{50}$ in the 0.032- 0.25µM range (**3d**, **3f**, **3g**, **3h**, **3i**, **3j**, **3k**, **3l**, **11a**, **11b** and **11c**). Dixon plot analysis of inhibition of compounds **3d**, **3h**, **11b** and **11c** confirmed the competitive mode of inhibition in the chemical series developed from the validated hit (**3a**) (Figure S2).

Of note, the compounds **3a**-**3o** contained a 2-hydroxyl-phenyl-hydrazone group, found in *Pan Assay Interference Compounds* because of possible interference in biological assays. Our experimental validation however ruled out non-specific inhibition due to formation of aggregates, spectroscopic properties, metal chelation or high reactivity (more details are given in the Supplementary Information, Text S2).

**Selectivity for *Sm*NACE over human CD38.** Compounds with IC$_{50}$ equal to or lower than 100 µM were tested *in vitro* on the human homolog of *Sm*NACE, namely CD38. The validated hit **3a** was not selective, nor did the micromolar inhibitors **3b** and **3c**. However, all derivatives with increased potency against *Sm*NACE were highly selective for the parasitic enzyme (**3d** – **3l**, **3o**, **4b** – **4c**, **11a** – **11b**). Importantly, the IC$_{50}$(CD38)/IC$_{50}$(*Sm*NACE) was greater than 1000 for seven out of eleven potent inhibitors of *Sm*NACE with IC$_{50}$ in the 0.032-0.25µM range (**3d**, **3g**, **3i**, **3j**, **3k**, **11b** and **11c**). Docking models of **3d** into *Sm*NACE and human CD38 suggested that the His / Trp sequence variation in the catalytic site, which is otherwise highly conserved, is the key structural determinant of the ligand selectivity (Figure S1).

CONCLUSION

Our approach to the discovery of new *Sm*NACE inhibitors combined docking using a homology model of *Sm*NACE and scoring using machine learning and interaction fingerprinting. We selected and experimentally tested 98 molecules on the recombinant enzyme, yielding a primary hit rate of about 10%. Only two compounds were validated: the natural product taxifolin and a new synthetic inhibitor. The two inhibitors are competitive and have ligand efficiency in the range of 0.30 kcal/mol/non-hydrogen atom. The synthesis of derivatives of the synthetic inhibitor allowed to improve by 3-log the inhibitor potency, while dramatically enhancing the selectivity for the parasitic enzyme *vs* the human homolog. The six best *Sm*NACE inhibitors (**3g**, **3i**, **3j**, **3k**, **11b** and **11c**) have IC$_{50}$ in the 0.032- 0.077µM range, corresponding to ligand efficiency of 0.46-0.54 kcal/mol/heavy atom. The compounds do not inhibit human CD38 at 100 µM concentration. These compounds are promising tools for the study of the *in vivo* function of *Sm*NACE, and its validation as a pharmacological target for antischistosomal therapy.

MATERIAL AND METHODS

**Homology modeling.** The three-dimensional structure of *Sm*NACE (UNIPROT: Q32TF5_SCHMA) was modeled by homology to human CD38 (PDB: 2pgj, chain A), bovine CD38 (PDB: 3gc6) and Aplysia cyclase (PDB: 1r15) and human BST1 (PDB: 1isj). The sequence alignment and the building of segments matching the ten structurally conserved regions (which include the full active site) were performed using the COMPOSER module of Sybyl (Tripos, Inc.). Loop construction was performed using COMPOSER if *Sm*NACE sequence was highly similar to the sequence of at least one of the templates otherwise using the automodel routine of Modeller (default setting). Six disulfide bridges were constrained during the modeling: C34-C48, C68-C144, C114-C120, C138-C152, C231-C252, C264-C273. *Sm*NACE model was energy minimized using Amber (University of California, San Francisco, CA, USA). The best model was chosen according to Procheck quality scores.

**Virtual screening.** The chemical library for virtual screening was obtained by merging commercial screening collections (from Asinex, Bionet, Chembridge ChemicalDivision, ChemStar, Enamine, InterBioScreen, lifeChemicals, MayBridge, OTAVA, Peakdale, Pharmeks, TimTec, Princeton and Vitas-M) then by the filtering of duplicates, reactive or non drug-like compounds, using Pipeline Pilot (Accelrys Software Inc, San Diego). The most probable ionization state of each molecule of the filtered library was predicted using Filter (OpenEye Scientific Software, Santa Fe). The 2D structures were converted into three-dimensional structures using Corina (Molecular Networks GmbH, Erlangen). The high-throughput docking of the chemical library was performed using Surflex v2.11 The docking site of *Sm*NACE was defined as the 41 residues surrounding the largest protein cavity in the model (Q100-M107, I110, R111, S122-E124, G129, F132- L135, W137, N159, V161-Q166,

A168-A170, Y172, A173, V182, N193, N195-E202) and represented by the protomol automatically generated from the coordinates of these residues using Surflex (setting on the adap_proto option). Each structure of the chemical library was docked into the protomol after an initial minimization of it coordinates (+premin). The conformational search involves five additional starting conformations (+multistart) and a maximum of 100 conformations per fragment (-maxconfs). The ten best poses were retained (-ndock_final) and refined by energy minimization (-remin). The minimal RMS difference between final poses was set to 0.5 (-divi_rms). The poses were selected according to docking scores (pKi $\geq$7.0, crash >-2 and polar $\geq$4.0), then filtered depending on their binding modes using a Naïve Bayes model generated with Weka 3.5.5 from a training set of 42 positive and 1540 negative reference binding modes described with residues-based interaction fingerprints.[18] The positive binding modes were extracted from the X-ray structures of complexes between human or bovine CD38 and a ligand (PDB: 2htc, 2i65, 2i66, 2i67, 2pqj, 2pgl, 3p5s and 3kou) after addition of hydrogen atoms using Sybyl (Tripos, Inc) and fragmentation of the ligand into phosphoribose, nucleoside and nucleotides monophosphate (or their fluorinated analogs). The negative binding modes were extracted from poses obtained by docking into *Sm*NACE (see above for detailed settings) of 89 molecules that were tested during a previous screening campaign and did not inhibit the enzyme at micromolar concentration.[10] Alternatively, a docked pose was retained if the direct comparison with any of the positive binding modes returned a Tanimoto coefficient greater or equal to 0.6. The chemical library was searched for close analogs of potential hits. Selected analogs had a Tanimoto coefficient computed from FCFP_4 fingerprint greater than 0.6 (Accelrys Software Inc, San Diego) and the same chemical scaffold as the parent molecule.

**Enzyme assays**. *Sm*NACE activity was determined by a sensitive continuous fluorometric assay using $1,N^6$-etheno $NAD^+$ ($\varepsilon$-$NAD^+$, Sigma) as substrate.[7,19] This assay consists in

measuring the appearance of the reaction product ε-ADP-ribose by the increase of fluorescence at $\lambda_{em}$ = 410 nm ($\lambda_{exc}$ = 310 nm) at 37 °C in 10 mM potassium phosphate buffer, pH 7.4, containing 0.05 % (w/v) emulphogen (100μl final volume) in a Spectramax Gemini XPS fluorescence plate reader (Molecular Devices). The effect of the inhibitors on the initial rates of the transformation of ε-NAD$^+$ was determined and IC$_{50}$ values were calculated from the plot of residual activity against the log of inhibitor concentration (6 data points) using a non-linear regression program (GraphPad, Prism). The type of inhibition was determined under the same experimental conditions using three different fixed inhibition concentrations and varying ε-NAD$^+$ concentrations. Alternatively, the enzyme activity was measured at 20 μM NAD$^+$ as described previously[7] by following the product formation by HPLC on a 300 x 3.9 mm μBondapack C18 column (Waters). The isocratic elution was performed at a flow rate of 1 mL/min (10 mM ammonium phosphate buffer, pH 5.5, with 1.2% (v/v) acetonitrile). In some cases [adenosine-U-$^{14}$C] NAD$^+$ ($2\times10^5$ dpm) was added to the unlabeled substrate. The eluted compounds were detected by absorbance recordings at 260 nm and by radiodetection (Flo-one, Packard Radiometric Instruments) when using [$^{14}$C] NAD$^+$.[7]

**Chemistry**

General experimental procedures: unless otherwise indicated, reactions were carried out under an atmosphere of argon in flame-dried glassware with magnetic stirring. Air and/or moisture-sensitive liquids were transferred *via* syringe. When required, solutions were degassed by bubbling argon through a needle. Organic solutions were concentrated by rotary evaporation at 25-60 °C at 15-30 torr. Analytical thin layer chromatography (TLC) was performed using plates cut from glass sheets (silica gel 60F-254 from Merck). Visualization was achieved under a 254 or 365 nm UV light and by immersion in an ethanolic solution of

1
2
3
4
5
6
7
8
9
10
11
12
13
14
15
16
17
18
19
20
21
22
23
24
25
26
27
28
29
30
31
32
33
34
35
36
37
38
39
40
41
42
43
44
45
46
47
48
49
50
51
52
53
54
55
56
57
58
59
60

cerium sulfate, followed by treatment with a heat gun. Column chromatography was carried

out as "Flash Chromatography" using silica gel G-25 (40-63 μM) from Macherey-Nagel.

Materials: All reagents were obtained from commercial sources and used without further

purifications. Dry MeOH and DMF were obtained from Aldrich.

Instrumentation: UV-Vis spectra and kinetic were recorded on Shimadzu UV-1800

spectrophotometer. IR spectra were recorded on a Nicolet 380 FT-IR spectrometer from

Thermo Electron Corporation as a $CH_2Cl_2$ solution or solid on a diamond plate. [1]H and [13]C

NMR spectra were recorded at 25 °C on Bruker 400 and 500 spectrometers. Recorded shifts

(δ) are reported in parts per million (ppm) and calibrated using residual undeuterated solvent.

Data are represented as follows: Chemical shift, mutiplicity (s = singlet, d = doublet, t =

triplet, q = quartet, quint = quintet, m = multiplet, br = broad), coupling constant (J, Hz) and

integration. High-resolution mass spectra (HRMS) were obtained using an Agilent Q-TOF

(time of flight) 6520 and low resolution mass spectra using an Agilent MSD 1200 SL

(ESI/APCI) with a Agilent HPLC1200 SL. The semi-preparative HPLC system consisted of a

Waters 600 pump, a 2487 detector (Waters), a 5 mL sample loop and a Sunfire C18 column

(150 mm × 19 mm i.d., 5 μm, Waters) with a 40 minutes gradient from 5% to 95%

acetonitrile.

**2-Methylfuran-3-carbohydrazide 2**
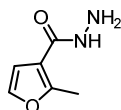


To a solution of methyl 2-methyl-3-furoate **1** (750 mg, 5.35 mmol, 1.0 eq) in MeOH (21

mL) was added hydrazine hydrate (2.68 g, 53.5 mmol, 10.0 eq.) and the resulting mixture

was heated to reflux for 16 h. The reaction mixture was concentrated under reduced pressure

and the crude solid was purified by silica gel column chromatography (*c*Hex/EtOAc 100% to

0% over 20 min) to afford 2-methylfuran-3-carbohydrazide **2** as a white solid (695 mg, 4.96

mmol, 93%).

^{1}H NMR (400 MHz, MeOD-d4) δ 7.25 (d, *J* = 2.01 Hz, 1H), 6.54 (d, *J* = 1.76 Hz, 1H),

2.42 (s, 3H), NH and $NH_2$ signals missing.

^{13}C NMR (100 MHz, MeOD-d4) δ 166.2, 157.8, 141.9, 115.2, 109.6, 13.4.

IR (film) 3272, 2330, 2341, 1635, 1512, 1337, 1216, 1048 cm^{-1}.

MS (ES+APCI) *m/z* 141 [M + H][+].


**General procedure for the synthesis of analogs 3a–3n:**

To a solution of **2** (1.0 eq) in EtOH was added aldehyde/ketone (1.0 eq) and the resulting

mixture was micro-irradiated for 5 to 10 min at 150 °C. The crude mixture was allowed to

cool down to room temperature. Water was added; the precipitate was collected, washed with

water and $Et_2O$ and dried under reduced pressure.


**(*Z*)-*N'*-(3,4-Dihydroxybenzylidene)-2-methylfuran-3-carbohydrazide 3a**
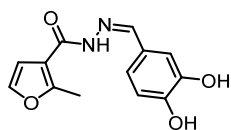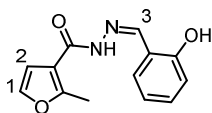


86%

[1]H (400 MHz, MeOD-d4) δ 8.12 (s, 1H), 7.43 (s, 1H), 7.31 (s, 1H), 7.37 (s, 1H), 7.05 (d, *J*

= 8.03 Hz, 1H), 6.89 – 6.70 (m, 2H), 2.62 (s, 3H), 2 OH and 1 NH signals missing.

[13]C (100 MHz, MeOD-d4) δ 163.0, 159.6, 150.1, 149.5, 146.9, 142.1, 127.6, 122.6, 116.3,

115.2, 114.2, 109.5, 13.7.

IR (film) 3295, 1607, 1495, 1372, 1298, 1281, 1190, 897, 724 cm^{-1}.

MS (ES+APCI) *m/z* 261 [M + H][+].

**(*Z*)-*N'*-(2-Hydroxybenzylidene)-2-methylfuran-3-carbohydrazide 3d**



*92%*

$^1$H (400 MHz, DMSO-d6) δ 11.64 (s, 1H, NH), 11.28 (s, 1H, OH), 8.57 (s, 1H, H-3), 7.61 (d, *J* = 2.0 Hz, 1H, H-1), 7.52 (d, *J* = 7.2 Hz, 1H, HAr), 7.29 (t, *J* = 7.2 Hz, 1H, HAr), 6.96 (d, *J* = 1.6 Hz, 1H, H-2), 6.95 – 6.91 (m, 2H, HAr), 2.56 (s, 3H, Me).

$^{13}$C (100 MHz, DMSO-d6) δ 159.1, 157.6, 157.4, 147.4, 141.1, 131.2, 129.5, 119.3, 118.7, 116.4, 113.9, 108.8, 13.3.

IR (film) 3523 (NH), 3296 (OH), 2359, 2337, 1627 (C=O), 1608 (C=C), 1495 (C=N), 1368, 1298, 1231, 1198, 897, 724 cm$^{-1}$.

MS (ES+APCI) *m/z* 245 [M + H]$^+$.

**(*Z*)-*N'*-(2-Methoxybenzylidene)-2-methylfuran-3-carbohydrazide 3e**



*52%*
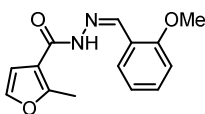
$^1$H (400 MHz, MeOD-d4) δ 8.71 (s, 1H), 8.09 (dd, *J* = 7.6, 1.2 Hz, 1H), 7.42 – 7.38 (m, 2H), 7.04 (d, *J* = 8.4 Hz, 1H), 6.99 (t, *J* = 7.6 Hz, 1H), 6.85 (d, *J* = 1.6 Hz, 1H), 3.89 (s, 3H), 2.60 (s, 3H), 1 NH signal missing.

$^{13}$C (100 MHz, MeOD-d4) δ 163.1, 159.9, 159.8, 145.5, 142.0, 132.9, 127.6, 123.8, 121.8, 115.1, 112.3, 109.5, 56.2, 13.7.

IR (film) 2350, 1633, 1601, 1428, 1350, 1232, 1014, 749, 732 cm$^{-1}$.

MS (ES+APCI) *m/z* 259 [M + H]$^+$.

**(*Z*)-*N'*-(3-Chloro-2-hydroxybenzylidene)-2-methylfuran-3-carbohydrazide 3f**
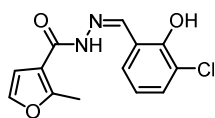


59%

[1]H (400 MHz, MeOD-d4) δ 8.44 (s, 1H), 7.45 (d, *J* = 1.6 Hz, 1H), 7.40 (dd, *J* = 8.0, 1.2 Hz, 1H), 7.33 (dd, *J* = 8.0, 1.6 Hz, 1H), 3.91 (t, *J* = 8.0 Hz, 1H), 6.84 (d, *J* = 1.2 Hz, 1H), 2.61 (s, 3H), 1 NH and 1 OH signals missing.

[13]C (100 MHz, MeOD-d4) δ 160.4 (2C), 155.2, 149.9, 142.2, 132.7, 130.4, 122.6 (2C), 120.9, 114.7, 109.3, 13.7.

IR (film) 3439, 3214, 2860, 1640, 1606, 1359, 1312, 1234, 1203, 1186, 1141, 1125, 936, 744 cm^{-1}.

MS (ES+APCI) *m/z* 279 [M + H]$^+$.

**(*Z*)-*N'*-(5-Chloro-2-hydroxybenzylidene)-2-methylfuran-3-carbohydrazide 3g**



55%
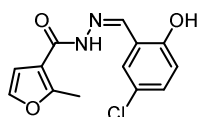
[1]H (400 MHz, MeOD-d4) δ 8.42 (s, 1H), 7.50 (d, *J* = 2.8 Hz, 1H), 7.44 (d, *J* = 2.0 Hz, 1H), 7.25 (dd, *J* = 8.8, 2.8 Hz, 1H), 6.90 (d, *J* = 8.8 Hz, 1H), 6.84 (d, *J* = 2.0 Hz, 1H), 2.60 (s, 3H), 1 NH and 1 OH signals missing.

[13]C (100 MHz, MeOD-d4) δ 162.5, 160.3, 157.9, 148.7, 142.2, 132.2, 130.2, 125.2, 121.2, 119.2, 114.8, 109.3, 13.7.

IR (film) 3420, 3202, 3050, 1640, 1606, 1556, 1486, 1353, 1321, 1286, 1238, 1210, 926, 732 cm$^{-1}$.

MS (ES+APCI) $m/z$ 279 [M + H]$^+$.

**(Z)-N'-(3-Fluoro-2-hydroxybenzylidene)-2-methylfuran-3-carbohydrazide 3h**



52%
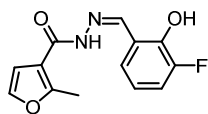
$^1$H (400 MHz, MeOD-d4) δ 8.48 (s, 1H), 7.44 (d, $J$ = 2.0 Hz, 1H), 7.26 (td, $J$ = 8.0, 1.6 Hz, 1H), 7.14 (ddd, $J$ = 11.1, 8.1, 2.1 Hz, 1H), 6.88 (td, $J$ = 8.0, 4.4 Hz, 1H), 6.84 (d, $J$ = 2.0 Hz, 1H), 2.61 (s, 3H), 1 NH and 1 OH signals missing.

$^{13}$C (100 MHz, MeOD-d4) δ 162.5, 160.2, 152.8 (d, $J$ = 241.0 Hz), 149.5, 147.3 (d, $J$ = 13.0 Hz), 142.2, 126.3 (d, $J$ = 2.5 Hz), 122.1 (d, $J$ = 2.7 Hz), 120.2 (d, $J$ = 7.0 Hz), 118.6 (d, $J$ = 18.2 Hz), 114.8, 109.3, 13.7.

$^{19}$F (376 MHz, MeOD-d4) δ -139.6 (dd, $J$ = 11.3, 5.5 Hz).

IR (film) 3426, 3214, 3030, 1633, 1607, 1473, 1365, 1246, 1235, 1124, 725 cm$^{-1}$.

MS (ES+APCI) $m/z$ 263 [M + H]$^+$.

**(Z)-N'-(2,4-Dichloro-6-hydroxybenzylidene)-2-methylfuran-3-carbohydrazide 3i**
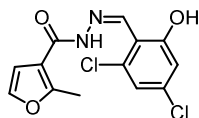


33%

$^1$H (400 MHz, MeOD-d4) δ 8.91 (s, 1H), 7.45 (d, $J$ = 2.0 Hz, 1H), 7.04 (d, $J$ = 2.0 Hz, 1H), 6.96 (d, $J$ = 2.0 Hz, 1H), 6.85 (d, $J$ = 1.6 Hz, 1H), 2.60 (s, 3H), 1 NH and 1 OH signals missing.

$^{13}$C (100 MHz, MeOD-d4) δ 161.7, 160.7 (2C), 146.8, 142.3, 137.9, 136.2, 121.4, 117.4, 115.7, 114.6, 109.3, 13.7.

IR (film) 3467, 3217, 3005, 1644, 1604, 1551, 1405, 1347, 1296, 1219, 1089, 953, 902, 830 cm$^{-1}$.

MS (ES+APCI) *m/z* 314 [M + H]$^+$.

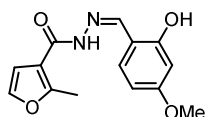**(Z)-N'-(2-Hydroxy-5-methoxybenzylidene)-2-methylfuran-3-carbohydrazide 3j**
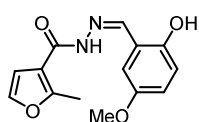
*47%*

$^1$H (400 MHz, MeOD-d4) δ 8.44 (s, 1H), 7.44 (d, *J* = 2.0 Hz, 1H), 7.05 (d, *J* = 2.8 Hz, 1H), 6.92 – 6.89 (m, 1H), 6.85 – 6.83 (m, 2H), 3.78 (s, 3H), 2.60 (s, 3H), 1 NH and 1 OH signals missing.

$^{13}$C (100 MHz, MeOD-d4) δ 162.4, 160.1, 154.2, 153.3, 150.1, 142.2, 119.8, 119.7, 118.4, 114.9, 114.4, 109.4, 56.3, 13.7.

IR (film) 3300, 3148, 2825, 1674, 1600, 1516, 1488, 1292, 1263, 1188, 1148, 1039, 858, 733 cm$^{-1}$.

MS (ES+APCI) *m/z* 275 [M + H]$^+$.

**(Z)-N'-(2-Hydroxy-4-methoxybenzylidene)-2-methylfuran-3-carbohydrazide 3k**

*60%*

<sup>1</sup>H (400 MHz, MeOD-d4) δ 8.37 (s, 1H), 7.43 (d, $J$ = 2.0 Hz, 1H), 7.27 (d, $J$ = 8.8 Hz, 1H), 6.82 (d, $J$ = 2.0 Hz, 1H), 6.53 – 6.48 (m, 2H), 3.81 (s, 3H), 2.59 (s, 3H), 1 NH and 1 OH signals missing.

<sup>13</sup>C (100 MHz, MeOD-d4) δ 164.4, 162.3, 161.3, 159.9, 151.1, 142.2, 133.0, 114.9, 112.9, 109.3, 107.7, 102.3, 55.9, 13.7.

IR (film) 3430, 3205, 1622, 1601, 1505, 1263, 1227, 1111, 964, 901, 731 cm<sup>-1</sup>.

MS (ES+APCI) $m/z$ 275 [M + H]<sup>+</sup>.

**(Z)-N'-(2-Hydroxy-4,6-dimethoxybenzylidene)-2-methylfuran-3-carbohydrazide 3l**
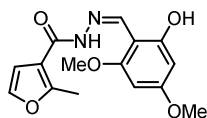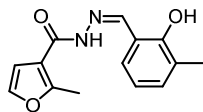


*68%*

<sup>1</sup>H (400 MHz, MeOD-d4) δ 8.75 (s, 1H), 7.42 (d, $J$ = 2.0 Hz, 1H), 6.82 (d, $J$ = 2.0 Hz, 1H), 6.12 (d, $J$ = 2.4 Hz, 1H), 6.09 (d, $J$ = 2.4 Hz, 1H), 3.85 (s, 3H), 3.80 (s, 3H), 2.58 (s, 3H), 1 NH and 1 OH signals missing.

<sup>13</sup>C (100 MHz, MeOD-d4) δ 165.4, 162.6, 162.0, 161.5, 159.7, 147.8, 142.1, 114.9, 109.4, 102.1, 94.8, 91.2, 56.3, 55.9, 13.7.

IR (film) 3018, 1629, 1599, 1347, 1306, 1215, 1145, 1110, 901, 812 cm<sup>-1</sup>.

MS (ES+APCI) $m/z$ 305 [M + H]<sup>+</sup>.

**(Z)-N'-(2-Hydroxy-3-methylbenzylidene)-2-methylfuran-3-carbohydrazide 3m**



*55%*

$^1$H (400 MHz, MeOD-d4) δ 8.40 (s, 1H), 7.44 (d, *J* = 2.0 Hz, 1H), 7.18 (d, *J* = 7.2 Hz, 1H), 7.15 (d, *J* = 4.6 Hz, 1H), 6.83 (d, *J* = 2.0 Hz, 1H), 6.83 (t, *J* = 7.6 Hz, 1H), 2.61 (s, 3H), 2.26 (s, 3H), 1 NH and 1 OH signals missing.

$^{13}$C (100 MHz, MeOD-d4) δ 160.3 (2C), 157.8, 151.8, 142.2, 133.8, 129.9, 126.9, 120.1, 118.5, 114.7, 109.3, 15.7, 13.7.

IR (film) 3449, 3320, 3069, 1639, 1606, 1552, 1404, 1363, 1304, 1261, 1020, 1053, 862, 731 cm$^{-1}$.

MS (ES+APCI) *m/z* 259 [M + H]$^+$.


**(*Z*)-*N'*-(3-(*tert*-Butyl)-2-hydroxybenzylidene)-2-methylfuran-3-carbohydrazide 3n**
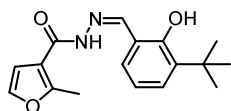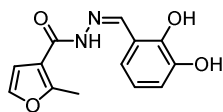


18%

$^1$H (400 MHz, MeOD-d4) δ 8.42 (s, 1H), 7.45 (d, *J* = 1.2 Hz, 1H), 7.33 (d, *J* = 7.2 Hz, 1H), 7.15 (d, *J* = 6.8 Hz, 1H), 6.88 – 6.84 (m, 2H), 2.61 (s, 3H), 1.45 (s, 9H), 1 NH and 1 OH signals missing.

$^{13}$C (100 MHz, MeOD-d4) δ 160.1 (2C), 158.7, 152.5, 142.2, 138.3, 130.6, 130.0, 119.9, 119.1, 114.8, 109.4, 35.8, 29.9 (3C), 13.7.

IR (film) 3439, 3236, 2955, 1640, 1605, 1433, 1313, 1232, 1203, 1126, 851, 742 cm$^{-1}$.

MS (ES+APCI) *m/z* 301 [M + H]$^+$.


**(*Z*)-*N'*-(2,3-Dihydroxybenzylidene)-2-methylfuran-3-carbohydrazide 3o**



52%

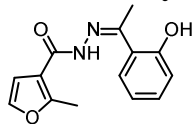[1]H (400 MHz, DMSO-d6) δ 11.64 (s, 1H), 11.11 (s, 1H), 9.19 (s, 1H), 8.53 (s, 1H), 7.61 (d,

$J$ = 1.6 Hz, 1H), 6.95 (d, $J$ = 1.2 Hz, 1H), 6.94 (d, $J$ = 6.2 Hz, 1H), 6.85 (dd, $J$ = 7.2, 0.7 Hz,

1H), 6.73 (t, $J$ = 8.0 Hz, 1H), 2.57 (s, 3H).

[13]C (100 MHz, DMSO-d6) δ 158.5, 157.0, 147.6, 145.5, 145.0, 140.5, 119.4, 118.5, 118.2,

116.7, 113.3, 108.2, 12.8.

IR (film) 3265, 3069, 1628, 1609, 1590, 1524, 1407, 1359, 1219, 950, 868 cm^{-1}.

MS (ES+APCI) $m/z$ 261 [M + H][+].

**(Z)-N'-(1-(2-Hydroxyphenyl)ethylidene)-2-methylfuran-3-carbohydrazide 3p**



43 %

[1]H (400 MHz, MeOD-d4) δ 7.61 (dd, $J$ = 8.0, 1.6 Hz, 1H), 7.44 (d, $J$ = 2.0 Hz, 1H), 7.28

(ddd, $J$ = 8.6, 6.7, 1.5 Hz, 1H), 6.93 – 6.87 (m, 2H), 6.89 (ddd, $J$ = 8.4, 6.9, 1.6 Hz, 1H), 2.59

(s, 3H), 2.46 (s, 3H), 1 NH and 1 OH signals missing.

[13]C (100 MHz, MeOD-d4) δ 163.1, 160.3, 160.0, 159.5, 142.1, 132.5, 129.4, 120.8, 119.8,

118.5, 115.3, 109.9, 13.8, 13.7.

IR (film) 3211, 2917, 1644, 1605, 1516, 1490, 1296, 1227, 1193, 1113, 829, 749 cm^{-1}.

MS (ES+APCI) $m/z$ 259 [M + H][+].

**2-Methylfuran-3-carboxylic acid 9**
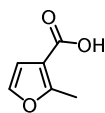


A solution of methyl 2-methyl-3-furoate (2.0 g, 14.3 mmol, 1.0 eq) in 20% NaOH (8 mL)

was heated to reflux for 2 h and further stirred for 48 h at room temperature. The resulting

mixture was allowed to cool down to room temperature before addition of 1N HCl under

vigorous stirring. The resulting precipitate was washed with water and dried under reduced pressure to give the desired carboxylic acid as a slightly yellow solid. The aqueous layer was extracted with $Et_2O$ (3 x 50 mL) and the combined organic layers were dried over $Na_2SO_4$ and concentrated under reduced pressure to give **9** as a slightly orange solid (1.54 g, 12.2 mmol, 86%).

$^1$H (400 MHz, CDCl$_3$) δ 7.26 (d, *J* = 2.0 Hz, 1H), 6.69 (d, *J* = 1.6 Hz, 1H), 2.61 (s, 3H), 1 COOH signal missing.

$^{13}$C (100 MHz, CDCl$_3$) δ 169.7, 161.1, 140.8, 113.0, 111.0, 14.0.

IR (film) 3040, 2885, 2578, 1670, 1590, 1436, 1300, 1125, 944, 735 cm$^{-1}$.

### *N*-(2-Methoxyphenethyl)-2-methylfuran-3-carboxamide 6
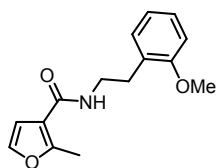


A mixture of 2-methylfuran-3-carboxylic acid (100 mg, 0.79 mmol, 1.0 eq.) and $Et_3N$ (275 µL, 1.98 mmol, 2.5 eq.) was dissolved in $CH_2Cl_2$ (3 mL). The resulting mixture was cooled down to 0 °C and ethyl chloroformate (83.4 µL, 0.87 mmol, 1.1 eq.) was added. The resulting mixture was stirred for 1 h before 2-methoxyphenethylamine (174.6 µL, 1.18 mmol, 1.5 eq.) was added. The solution was warmed up to room temperature and stirred for 24 h. $H_2O$ was added and the layers were separated. The aqueous layer was extracted with $CH_2Cl_2$ (3 x 5 mL) and the combined organic layers were dried over $Na_2SO_4$ and concentrated under reduced pressure. The crude material was purified by preparative reverse phase HPLC (SunFire column, acidic gradients with MeCN-$H_2O$ containing 0.05 % TFA) to give **6** as a white solid (200 mg, 0.77 mmol, 97%).
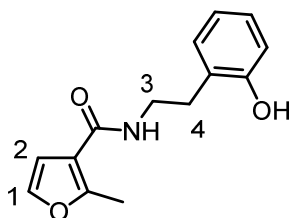
¹H (400 MHz, MeOD-d4) δ 7.33 (d, *J* = 2.0 Hz, 1H), 7.18 (t, *J* = 8.0 Hz, 1H), 6.82 – 6.80 (m, 2H), 6.77 – 6.76 (m, 1H), 6.62 (d, *J* = 2.0 Hz, 1H), 3.51 (t, *J* = 7.4 Hz, 2H), 3.76 (s, 3H), 2.84 (t, *J* = 7.4 Hz, 2H), 2.49 (s, 3H), 1 NH signal missing.

¹³C (100 MHz, MeOD-d4) δ 166.5, 161.3, 157.7, 142.2, 141.7, 130.4, 122.2, 116.9, 115.4, 112.9, 109.9, 55.5, 42.0, 36.75, 13.4.

IR (film) 3355, 2478, 2071, 1626, 1602, 1487, 1463, 1260, 970 cm$^{-1}$.

MS (ES+APCI) *m/z* 260 [M + H]$^{+}$.

**N-(2-Hydroxyphenethyl)-2-methylfuran-3-carboxamide 5**



To a solution of *N*-(2-hydroxyphenethyl)-2-methylfuran-3-carboxamide **6** (25 mg, 0.09 mmol, 1.0 eq.) in $CH_2Cl_2$ (500 µL) was added at −78 °C BBr$_3$ (10.9 µL, 0.11 mmol, 1.2 eq.) and the resulting mixture was stirred at −78 °C for 1 h before warming up to room temperature. $H_2O$ was added and the resulting mixture was stirred for 15 min. The layers were separated and the aqueous layer was extracted with $CH_2Cl_2$ (3 x 5 mL). The combined organic layers were dried over $Na_2SO_4$ and concentrated under reduced pressure. The crude material was purified by preparative reverse phase HPLC (SunFire column, acidic gradients with MeCN-$H_2O$ containing 0.05 % TFA) to give **5** as a white solid (13.5 mg, 0.05 mmol, 57%).

¹H (400 MHz, MeOD-d4) δ 7.33 (d, *J* = 1.6 Hz, 1H, H-1), 7.09 (t, *J* = 7.8 Hz, 1H, HAr), 6.70 (d, *J* = 8.0 Hz, 1H, HAr), 6.68 (br s, 1H, HAr), 6.64 – 6.62 (m, 1H, HAr), 6.62 (d, *J* =
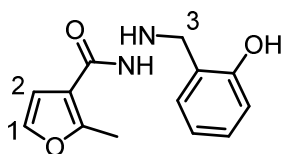
2.0 Hz, 1H, H-2), 3.49 (t, *J* = 7.6 Hz, 2H, H-3), 2.79 (t, *J* = 7.4 Hz, 2H, H-4), 2.50 (s, 3H,

Me), 1 NH and 1 OH signals missing.

$^{13}$C (100 MHz, MeOD-d4) δ 160.4, 158.6, 157.7, 142.1, 141.7, 140.2, 130.5, 121.0, 116.7,

114.2, 109.1, 42.1, 36.7, 13.4.

IR (film) 3322 (NH), 2200, 1663 (C=O), 1635 (C=C), 1524 (C=N), 1406, 1216, 1140 cm$^{-1}$.

MS (ES+APCI) *m/z* 246 [M + H]$^+$.
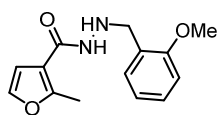
**N'-(2-Hydroxybenzyl)-2-methylfuran-3-carbohydrazide 4b**



To a solution of (*Z*)-*N*'-(2-hydroxybenzylidene)-2-methylfuran-3-carbohydrazide **3b** (25 mg, 0.10

mmol, 1.0 eq.) in TFA (152 µL) at 0 °C was added Et$_3$SiH (33 µL, 0.20 mmol, 2.0 eq.) and the

resulting mixture was stirred at 0 °C for 4 h. The crude mixture was diluted in toluene and

concentrated under reduced pressure. The crude material was purified by preparative reverse phase

HPLC (SunFire column, acidic gradients with MeCN-H$_2$O containing 0.05 % TFA) to give **4b** as a

white solid (20 mg, 0.08 mmol, 79%).

$^1$H (400 MHz, MeOD-d4) δ 7.41 (s, 1H, H-1), 7.30 – 7.24 (m, 2H, HAr), 6.90 – 6.85 (m,

2H, HAr), 6.65 (s, 1H, H-2), 4.40 (s, 2H, H-3), 2.54 (s, 3H, Me), 2 NH and 1 OH signals

missing.

$^{13}$C (100 MHz, MeOD-d4) δ 164.2, 160.2, 158.0, 142.5, 132.9, 132.2, 120.8, 118.6, 116.3,

113.5, 109.3, 52.2, 13.5.

IR (film) 3495 (NH), 3247 (OH), 2353, 1671 (C=O), 1606 (C=C), 1460 (C=N), 1235,

1200, 1138, 754 cm$^{-1}$.

MS (ES+APCI) *m/z* 247 [M + H]$^+$.
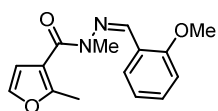
### N'-(2-Methoxybenzyl)-2-methylfuran-3-carbohydrazide 4c



To a solution of (Z)-N'-(2-methoxybenzylidene)-2-methylfuran-3-carbohydrazide **3c** (22 mg, 0.08 mmol, 1.0 eq.) in TFA (126 µL) at 0 °C was added Et$_3$SiH (27 µL, 0.20 mmol, 2.0 eq.) and the resulting mixture was stirred at 0 °C for 4 h. The crude mixture was diluted in toluene and concentrated under reduced pressure. The crude material was purified by preparative reverse phase HPLC (SunFire column, acidic gradients with MeCN-H$_2$O containing 0.05 % TFA) to give **4c** as a white solid (16.6 mg, 0.06 mmol, 75%).

[1]H (400 MHz, MeOD-d4) δ 7.42 (td, J = 7.6, 1.6 Hz, 1H), 7.41 (d, J = 2.0 Hz, 1H), 7.35 (dd, J = 7.6, 1.6 Hz, 1H), 7.06 (d, J = 8.4 Hz, 1H), 6.98 (td, J = 7.6, 1.2 Hz, 1H), 6.12 (d, J = 2.0 Hz, 1H), 4.36 (s, 2H), 3.90 (s, 3H), 2.53 (s, 3H), 2 NH signals missing.

[13]C (100 MHz, MeOD-d4) δ 164.1, 159.9, 159.8, 142.4, 132.9, 132.2, 121.8, 121.1, 113.7, 111.9, 109.2, 56.1, 51.9, 13.5.

IR (film) 3290, 1667, 1604, 1494, 1485, 1438, 1246, 1200, 1133, 1027, 753 cm$^{-1}$.

MS (ES+APCI) m/z 261 [M + H]$^+$.

### (Z)-N'-(2-Methoxybenzylidene)-N,2-dimethylfuran-3-carbohydrazide 8



To a suspension of NaH (13.9 mg, 0.35 mmol, 1.2 eq.) in dry THF (1.0 mL) was added (Z)-N'-(2-methoxybenzylidene)-2-methylfuran-3-carbohydrazide **3e** (75 mg, 0.29 mmol, 1.0 eq.) and the resulting mixture was heated under reflux for 1 h. CH$_3$I (18.1 µL, 0.29 mmol, 1.0 eq.) in THF (200 µL) was added and the reaction mixture was further heated under reflux for 1 h. The crude mixture was cooled down to room temperature and concentrated under reduced pressure. The crude material was purified by preparative reverse phase HPLC (SunFire

column, acidic gradients with MeCN-$H_2O$ containing 0.05 % TFA) to give **8** as a white solid (55.4 mg, 0.20 mmol, 70%).

$^1$H (400 MHz, MeOD-d4) δ 8.21 (s, 1H), 7.46 (dd, $J$ = 8.0, 2.0 Hz, 1H), 7.38 (d, $J$ = 2.0 Hz, 1H), 7.36 (ddd, $J$ = 8.4, 7.3, 1.9 Hz, 1H), 7.05 (dd, $J$ = 8.4, 0.8 Hz, 1H), 6.94 (t, $J$ = 7.4 Hz, 1H), 6.81 (d, $J$ = 2.0 Hz, 1H), 3.91 (s, 3H), 3.48 (d, $J$ = 0.4 Hz, 3H), 2.45 (s, 3H).

$^{13}$C (100 MHz, MeOD-d4) δ 168.1, 159.7, 158.8, 140.6, 137.7, 132.2, 126.9, 124.4, 121.8, 116.8, 114.1, 112.5, 56.1, 28.7, 13.9.

IR (film) 2917, 1647, 1601, 1413, 1333, 1246, 1620, 1017, 732 cm$^{-1}$.

MS (ES+APCI) $m/z$ 273 [M + H]$^+$.

**(Z)-N'-(2-Hydroxybenzylidene)-N,2-dimethylfuran-3-carbohydrazide 7**
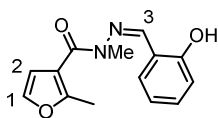


To a solution of (*Z*)-*N'*-(2-Methoxybenzylidene)-*N*,2-dimethylfuran-3-carbohydrazide **8** (18.9 mg, 0.06 mmol, 1.0 eq.) in $CH_2Cl_2$ (500 µL) at −78 °C was added BBr$_3$ (7.8 µL, 0.08 mmol, 1.2 eq.) and the resulting mixture was stirred at −78 °C for 1 h before warming up to room temperature. $H_2O$ was added and the resulting mixture was stirred for 15 min. The layers were separated and the aqueous layer was extracted with $CH_2Cl_2$ (3 x 5 mL). The combined organic layers were dried over $Na_2SO_4$ and concentrated under reduced pressure. The crude material was purified by preparative reverse phase HPLC (SunFire column, acidic gradients with MeCN-$H_2O$ containing 0.05 % TFA) to give **7** as a white solid (9.8 mg, 0.04 mmol, 55%).
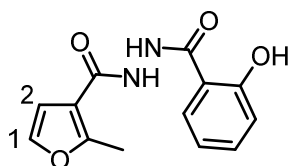
$^1$H (400 MHz, MeOD-d4) δ 8.20 (s, 1H, H-3), 7.46 (dd, $J$ = 7.5, 2.0 Hz, 1H, HAr), 7.44 (d, $J$ = 2.0 Hz, 1H, H-1), 7.24 (ddd, $J$ = 8.4, 7.5, 1.8 Hz, 1H, HAr), 6.90 (td, $J$ = 7.8, 1.2 Hz, 1H,

HAr), 6.82 (dd, *J* = 8.4, 0.8 Hz, 1H, HAr), 6.63 (d, *J* = 2.0 Hz, 1H, H-2), 3.25 (d, *J* = 0.4 Hz,

3H, N-Me), 2.39 (s, 3H, Me), 1 OH signal missing.

$^{13}$C (100 MHz, MeOD-d4) δ 167.9, 158.3, 156.9, 144.6, 141.8, 132.3, 131.7, 120.7, 120.1,

117.4, 116.6, 112.3, 28.7, 13.8.

MS (ES+APCI) *m/z* 259 [M + H]$^+$.

**_N'_-(2-Hydroxybenzoyl)-2-methylfuran-3-carbohydrazide 11a**



To a solution of salicylhydrazide (161.4 mg, 1.06 mmol, 1.0 eq.) in THF (5 mL) at 0 °C

was added Et$_3$N (222 µL, 1.59 mmol, 1.5 eq.) and the resulting mixture was stirred at 0 °C for

15 min. To this mixture was added 2-methylfuran-3-carbonyl chloride (230 mg, 1.59 mmol,

1.0 eq.) in THF (1 mL) and the resulting mixture was stirred for 15 min at 0 °C, allowed to

warm up to room temperature and further stirred for 12 h. The crude mixture was diluted with

water and the aqueous layer was extracted with EtOAc. The combined organic layers were

dried over MgSO$_4$ and concentrated under reduced pressure. The crude material was

triturated with MeOH. The solid was filtered off, washed with cold MeOH and dried under

reduced pressure to give **11a** as a white solid (117 mg, 0.45 mmol, 42%).

$^1$H (400 MHz, MeOD-d4) δ 7.88 (dd, *J* = 7.8, 1.6 Hz, 1H, HAr), 7.43 (ddd, *J* = 8.2, 7.3, 1.8

Hz, 1H, HAr), 7.42 (d, *J* = 2.1 Hz, 1H, H-1), 6.96 – 6.92 (m, 2H, HAr), 6.80 (d, *J* = 2.0 Hz,

1H, H-2), 2.57 (s, 3H, Me), 2 NH and 1 OH signals missing.

$^{13}$C (100 MHz, MeOD-d4) δ 169.8, 165.4, 160.8, 159.4, 142.1, 135.3, 129.5, 120.4, 118.4,

115.9, 114.7, 109.7, 13.5.

IR (film) 3221 (NH), 3005 (OH), 1650 (C=O), 1632 (C=N), 1594, 1523, 1487, 1308, 1213,

1160, 729 cm$^{-1}$.

MS (ES+APCI) $m/z$ 259 [M − H]$^+$.

**General procedure for the synthesis of analogs 11b–11d:**

To a solution of 2-methylfuran-3-carbohydrazide **2** (1.0 eq.) in THF (5 mL) at 0 °C was added Et$_3$N (1.5 eq.) and the resulting mixture was stirred at 0 °C for 15 min. To this mixture was added acid chloride derivative (1.0 eq.) in THF (1 mL) and the resulting mixture was stirred for 15 min at 0 °C, allowed to warm up to room temperature and further stirred for 12 h. The crude mixture was diluted with water and the aqueous layer was extracted with EtOAc. The combined organic layers were dried over MgSO$_4$ and concentrated under reduced pressure. The crude material was triturated with MeOH. The solid was filtered off, washed with cold MeOH and dried under reduced pressure.

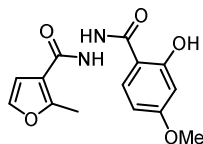**$N'$-(5-Chloro-2-hydroxybenzoyl)-2-methylfuran-3-carbohydrazide 11b**



25%
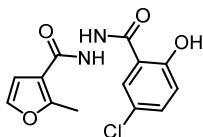
$^1$H (400 MHz, MeOD-d4) δ 7.90 (d, $J$ = 2.8 Hz, 1H), 7.43 (t, $J$ = 2.2 Hz, 1H), 7.41 (d, $J$ = 2.8 Hz, 1H), 6.96 (d, $J$ = 8.8 Hz, 1H), 2.0 Hz, 1H), 2.57 (s, 3H), 2 NH and 1 OH signals missing.

IR (film) 3310, 1667, 1608, 1538, 1481, 1421, 1283, 1234, 1123, 824 cm$^{-1}$.

MS (ES+APCI) $m/z$ 293 [M − H]$^+$.

**$N'$-(2-Hydroxy-4-methoxybenzoyl)-2-methylfuran-3-carbohydrazide 11c**

*16%*

$^1$H (400 MHz, MeOD-d4) δ 7.44 (d, *J* = 3.2 Hz, 1H), 7.42 (d, *J* = 2.4 Hz, 1H), 7.05 (dd, *J* = 8.8, 3.2 Hz, 1H), 6.89 (d, *J* = 8.8 Hz, 1H), 6.80 (d, *J* = 1.6 Hz, 1H), 3.79 (s, 3H), 2.57 (s, 3H), 2 NH and 1 OH signals missing.

$^{13}$C (100 MHz, MeOD-d4) δ 169.3, 165.3, 159.4, 154.6, 154.0, 142.1, 122.7, 119.3, 115.9, 114.7, 112.8, 109.7, 56.3, 13.6.

IR (film) 3218, 3003, 2358, 1745, 1635, 1590, 1300, 763 cm$^{-1}$.

MS (ES+APCI) *m/z* 289 [M − H]$^+$.

### *N'*-(2-Hydroxy-3-methylbenzoyl)-2-methylfuran-3-carbohydrazide 11d



*25%*
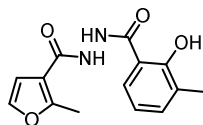
$^1$H (400 MHz, MeOD-d4) δ 7.64 (dd, *J* = 8.0, 0.8 Hz, 1H), 7.42 (d, *J* = 2.0 Hz, 1H), 7.33 – 7.31 (m, 1H), 6.81 (t, *J* = 7.6 Hz, 1H), 6.80 (d, *J* = 2.0 Hz, 1H), 2.57 (s, 3H), 2.23 (s, 3H), 2 NH and 1 OH signals missing.

$^{13}$C (100 MHz, MeOD-d4) δ 171.8, 165.7, 160.8, 159.4, 142.1, 136.3, 128.0, 125.6, 119.4, 114.7, 113.7, 109.7, 15.8, 13.6

IR (film) 3212, 3011, 2358, 1743, 1626, 1607, 1505, 1298, 1099, 899 cm$^{-1}$.

MS (ES+APCI) *m/z* 293 [M − H]$^+$.

**General procedure for the synthesis of analogs 12a–12d:**

To a solution of intermediates **11a**–**11c** (1.0 eq.) and 2-chloro-1,3-dimethylimidazolinium chloride (1.0 eq) in $CH_2Cl_2$ (2 mL)was added $Et_3N$ (2.0 eq.) and the resulting mixture was stirred at room temperature for 12 h. The crude material was purified by preparative reverse phase HPLC (SunFire column, acidic gradients with MeCN-$H_2O$ containing 0.05 % TFA).

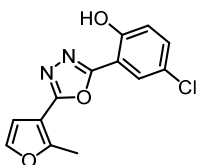**2-(5-(2-Methylfuran-3-yl)-1,3,4-oxadiazol-2-yl)phenol 12a**
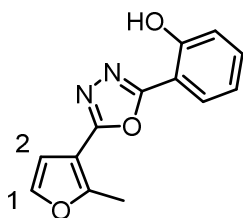


*65%*

[1]H (400 MHz, MeOD-d4) δ 7.88 (dd, *J* = 8.0, 1.6 Hz, 1H, HAr), 7.57 (d, *J* = 2.0 Hz, 1H, H-1), 7.49 – 7.45 (m, 1H, HAr), 7.10 – 7.04 (m, 2H, HAr), 6.93 (d, *J* = 2.0 Hz, 1H, H-2), 2.72 (s, 3H, Me), 1 OH signal missing.

[13]C (100 MHz, MeOD-d4) δ 164.7, 161.2, 158.5, 156.9, 143.7, 134.7, 128.4, 121.1, 118.2, 110.2, 109.8, 107.2, 13.7.

IR (film) 3216 (OH), 2919, 1623 (C=C), 1486 (C=N), 1254, 739 cm^{-1}.

MS (ES+APCI) *m/z* 243 [M +H][+].

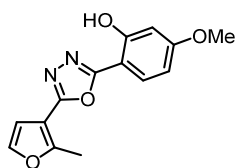**4-Chloro-2-(5-(2-methylfuran-3-yl)-1,3,4-oxadiazol-2-yl)phenol 12b**



*39%*

[1] H (400 MHz, MeOD-d4) δ 77.86 (d, *J* = 2.0 Hz, 1H), 7.57 (d, *J* = 1.6 Hz, 1H), 7.44 (dd, *J* = 8.0, 3.2 Hz, 1H), 7.09 (d, *J* = 7.2 Hz, 1H), 6.94 (d, *J* 1.6 Hz, 1H), 2.72 (s, 3H), 1 OH signal missing.

IR (film) 3216, 2919, 1625, 1585, 1297, 1235, 826, 721cm^{-1}.

MS (ES+APCI) *m/z* 277 [M + H][+].

**5-Methoxy-2-(5-(2-methylfuran-3-yl)-1,3,4-oxadiazol-2-yl)phenol 12c**



*45%*

[1] H (400 MHz, MeOD-d4) δ 7.56 (d, *J* = 1.6 Hz, 1H), 7.34 (d, *J* = 2.4 Hz, 1H), 7.08 (dd, *J* = 7.2, 2.4 Hz, 1H), 7.01 (d, *J* = 7.2 Hz, 1H), 6.93 (d, *J* = 1.6 Hz, 1H), 3.83 (s, 3H), 2.72 (s, 3H), 1 OH signal missing.

[13] C (100 MHz, MeOD-d4) δ 164.6, 161.2, 156.9, 154.4, 152.7, 143.6, 121.7, 119.3, 111.5, 110.2, 109.5, 107.1, 56.4, 13.7.

IR (film) 3216, 2919, 2359, 1625, 1487, 1236, 1125, 735 cm^{-1}.

MS (ES+APCI) *m/z* 273 [M + H][+].

1
2
3
4
5
6
7
8
9
10
11
12
13
14
15
16
17
18
19
20
21
22
23
24
25
26
27
28
29
30
31
32
33
34
35
36
37
38
39
40
41
42
43
44
45
46
47
48
49
50
51
52
53
54
55
56
57
58
59
60

FIGURES

**Figure 1.** Schematic overview of the virtual screening protocol.

**Figure 2**. Inhibition of *Sm*NACE by **3a** *in vitro*. (a) Structure of the inhibitor identified by virtual screening. (b) Concentration-dependent inhibition of recombinant *Sm*NACE, determined fluorometrically using $1,N^6$-etheno $NAD^+$ as substrate. Residual enzyme activity is plotted as a function of the log of inhibitor concentration and analyzed by non-linear regression. (c) Reciprocals of the initial velocities (1/v) are plotted against a series of inhibitor concentrations [I], at substrate concentrations equal to 20 µM, 50 µM and 100 µM.

1
2
3 SCHEMES
4
5
6 **Scheme 1.** Synthesis of hydrazide derivatives[a]
7
8
9 [a] Reagents and conditions: (a) $N_2H_4.H_2O$, MeOH, 75 °C, 12 h, 99%; (b) aldehyde or ketone,
10 EtOH, 150 °C, 5-10 min, μW, 18 – 92%; (c) $Et_3SiH$, TFA, 0 °C, 4 h, 79% for **4b** and 75% for
11 **4c**; (d) MeI, NaH, THF, 80 °C, 2 h, 70%. (e) $BBr_3$, $CH_2Cl_2$, −78 °C to rt, 12 h, 55%.
12
13
14
15 **Scheme 2.** Synthesis of amide derivatives **5** and **6**[a]
16
17
18 [a] Reagents and conditions: (a) NaOH, $H_2O$, reflux, 12 h, 86%; (b) $Et_3N$, ethyl
19 chloroformate, 2-(2-methoxyphenyl)ethan-1-amine, $CH_2Cl_2$, 0 °C to rt, 12 h, 97%; (c) $BBr_3$,
20 $CH_2Cl_2$, −78 °C to rt, 12 h, 57%.
21
22
23
24 **Scheme 3.** Synthesis of bis-amide **11a**–**11d** and 1,3,4-oxadiazole derivatives **12a**–**12d**[a]
25
26
27 [a] Reagents and conditions: (a) i) $(COCl)_2$, DMF, THF, 0 °C to rt, 2 h, ii) $Et_3N$, $CH_2Cl_2$, **10-
28 2**, 0 °C to rt, 12 h, 16 – 19%; (b) 2-chloro-1,3-dimethylimidazolinium chloride, $Et_3N$,
29 $CH_2Cl_2$, rt, 12 h, 39 – 65%.
30
31
32
33
34
35
36
37
38
39
40
41
42
43
44
45
46
47
48
49
50
51
52
53
54
55
56
57
58
59
60

1
2
3 TABLES
4
5
6 **Table 1**. Inhibition of *Sm*NACE and human CD38[b]
7
8
9 [a]*In vitro* assay. The given $IC_{50}$ values are the means of three independent determinations
10 using the fluorimetric assay for compounds **3a**-**3e**; [b]NS = Not soluble; NA = Not active (0%
11 inhibition at 100 µM); PI = Percent of inhibition of human CD38 at 100 µM as measured
12 using the HPLC assay; NT = Not tested (PI were not determined if $IC_{50(SmNACE)}$ > 100 µM or
13 if $IC_{50(hCD38)}$ were determined, $IC_{50}$ were not determined if no inhibition was observed at 100
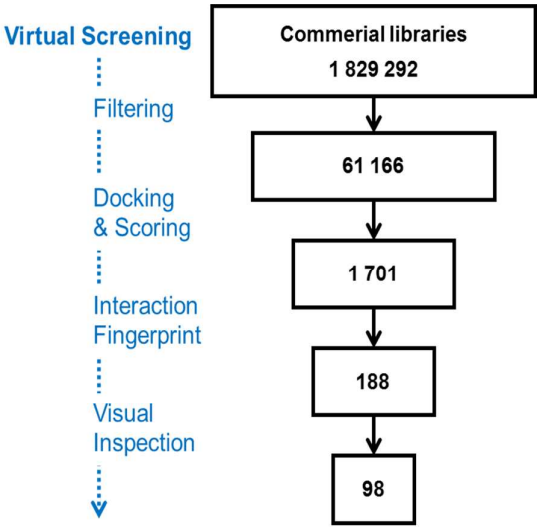14 µM). [c]The Z-isomeric form of hydrazone was suggested by docking studies (Figure S1).
15
16
17
18
19
20
21
22
23
24
25
26
27
28
29
30
31
32
33
34
35
36
37
38
39
40
41
42
43
44
45
46
47
48
49
50
51
52
53
54
55
56
57
58
59
60

**Figure 1.** Schematic overview of the virtual screening protocol.
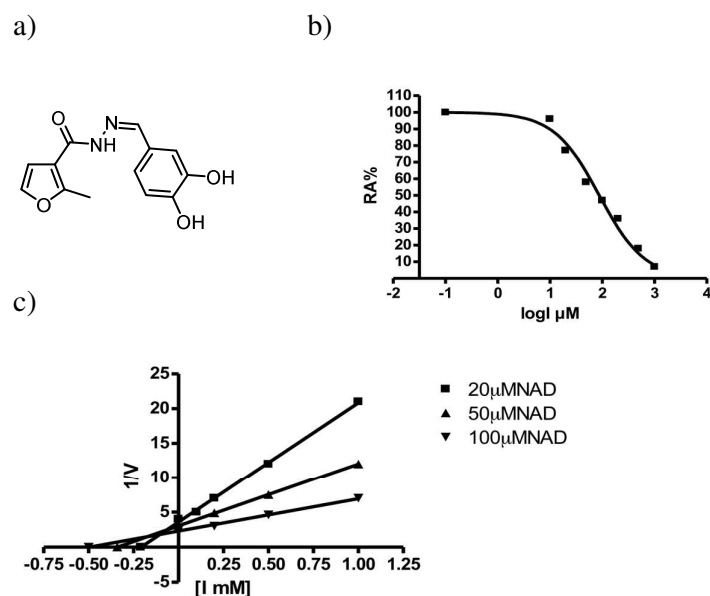
a)             b)

c)



**Figure 2**. Inhibition of *Sm*NACE by **3a** *in vitro*. (a) Structure of the inhibitor identified by virtual screening. The Z-isomeric form of hydrazone was suggested by docking studies (Figure S1). (b) Concentration-dependent inhibition of recombinant *Sm*NACE, determined fluorometrically using $1,N^6$-etheno NAD$^+$ as substrate. Residual enzyme activity is plotted as a function of the log of inhibitor concentration and analyzed by non-linear regression. (c) Reciprocals of the initial velocities (1/v) are plotted against a series of inhibitor concentrations [I], at substrate concentrations equal to 20 µM, 50 µM and 100 µM.
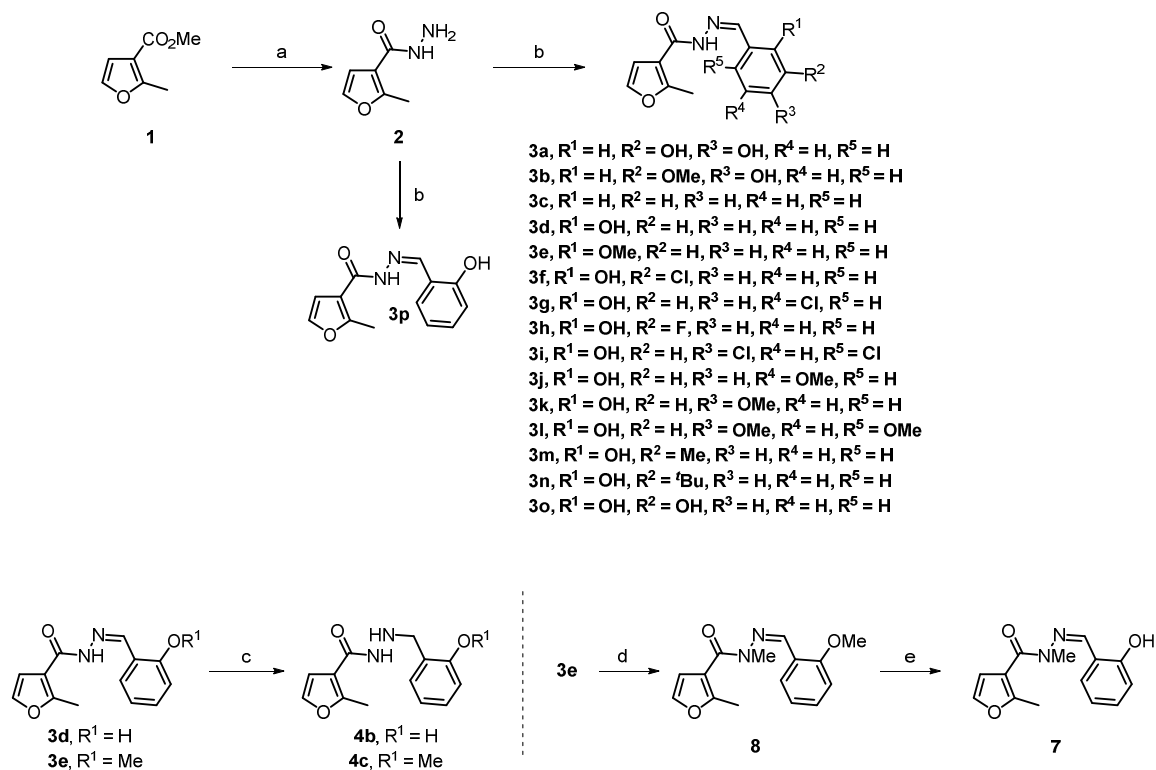
**Scheme 1.** Synthesis of hydrazide derivatives[a]

[a] Reagents and conditions: (a) $N_2H_4 \cdot H_2O$, MeOH, 75 °C, 12 h, 99%; (b) aldehyde or ketone, EtOH, 150 °C, 5-10 min, μW, 18 – 92%; (c) $Et_3SiH$, TFA, 0 °C, 4 h, 79% for **4b** and 75% for **4c**; (d) MeI, NaH, THF, 80 °C, 2 h, 70%. (e) $BBr_3$, $CH_2Cl_2$, −78 °C to rt, 12 h, 55%.
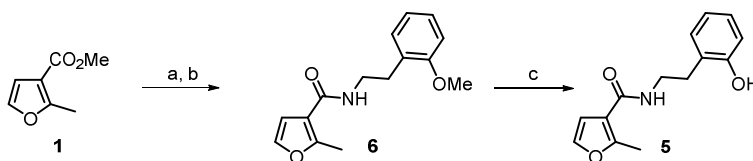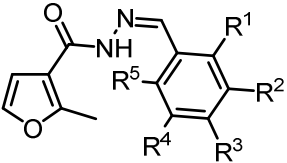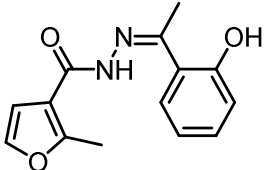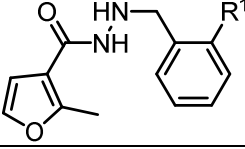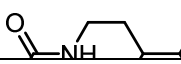
**Scheme 2.** Synthesis of amide derivatives **5** and **6**[a]

[a] Reagents and conditions: (a) NaOH, H$_2$O, reflux, 12 h, 86%; (b) Et$_3$N, ethyl chloroformate, 2-(2-methoxyphenyl)ethan-1-amine, CH$_2$Cl$_2$, 0 °C to rt, 12 h, 97%; (c) BBr$_3$, CH$_2$Cl$_2$, −78 °C to rt, 12 h, 57%.
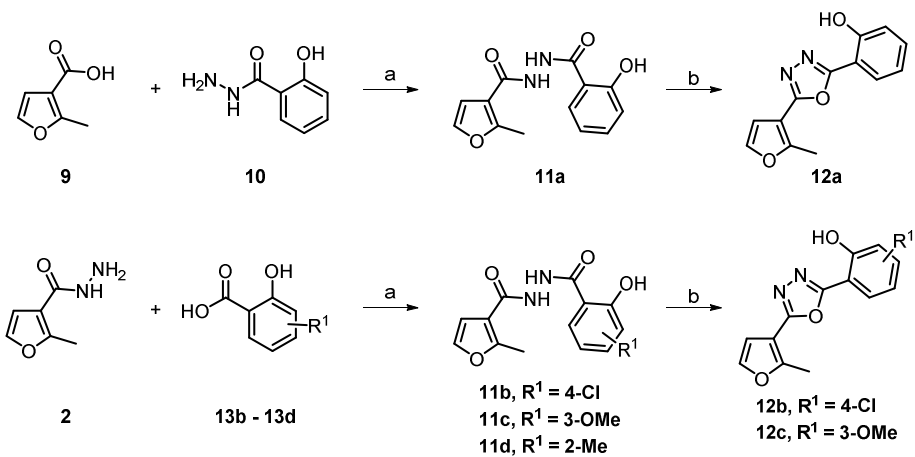
**Scheme 3.** Synthesis of bis-amide **11a–11d** and 1,3,4-oxadiazole derivatives **12a–12d**[a]

[a] Reagents and conditions: (a) i) (COCl)$_2$, DMF, THF, 0 °C to rt, 2 h, ii) Et$_3$N, CH$_2$Cl$_2$, **10-2**, 0 °C to rt, 12 h, 16 – 19%; (b) 2-chloro-1,3-dimethylimidazolinium chloride, Et$_3$N, CH$_2$Cl$_2$, rt, 12 h, 39 – 65%.

| # | Scaffold[c] | $R^1$ | $R^2$ | $R^3$ | $R^4$ | $R^5$ | *Sm*NACE IC$_{50}$ (μM) | hCD38 IC$_{50}$ (μM) | hCD38 PI (%) |
|---|---|---|---|---|---|---|---|---|---|
| 3a | | H | OH | OH | H | H | 88 ±8 | 109 ±18 | NT |
| 3b | | H | OMe | OH | H | H | 80 ±12 | 103 ±19 | NT |
| 3c | | H | H | H | H | H | 330 ±28 | 296 ±45 | NT |
| 3d | | OH | H | H | H | H | 0.13 ±0.03 | 430 ±75 | 20.0 |
| 3e | | OMe | H | H | H | H | 67 ±11 | NT | 0 |
| 3f | | OH | Cl | H | H | H | 0.15 ±0.09 | 14 ±2 | 66.7 |
| 3g | | OH | H | H | Cl | H | 0.033 ±0.005 | NT | 0 |
| 3h |  | OH | F | H | H | H | 0.036 ±0.0045 | 26 ±2.6 | 27.2 |
| 3i | | OH | H | Cl | H | Cl | 0.077 ±0.01 | NT | 0 |
| 3j | | OH | H | H | OMe | H | 0.045 ±0.004 | NT | 0 |
| 3k | | OH | H | OMe | H | H | 0.032 ±0.002 | NT | 0 |
| 3l | | OH | H | OMe | H | OMe | 0.19 ±0.02 | NT | 0 |
| 3m | | OH | Me | H | H | H | 59 ±0.8 | NT | 0 |
| 3n | | OH | *t*Bu | H | H | H | 105 ±9.5 | NT | NT |
| 3o | | OH | OH | H | H | H | 8.7 ±2 | NT | 0 |
| 3p |  | | | | | | NS | NT | NT |
| 4b |  | OH | H | H | H | H | 12.3 ±0.8 | NT | 0 |
| 4c | | OMe | H | H | H | H | 11.6 ±0.9 | NT | 0 |
| 5 |  | OH | H | H | H | H | 131 ±15.6 | NT | NT |

| | | | | | | | | | |
|---|---|---|---|---|---|---|---|---|---|
| **6** | | OMe | H | H | H | H | NA | NT | NT |
| **7** |  | OH | H | H | H | H | NS | NT | NT |
| **8** | | OMe | H | H | H | H | 513 ±80 | NT | NT |
| **11a** |  | OH | H | H | H | H | 0.25 ±0.04 | 120 ±8 | 27.6 |
| **11b** | | OH | H | H | Cl | H | 0.039 ±0.005 | NT | 6.7 |
| **11c** | | OH | H | OMe | H | H | 0.074 ±0.004 | NT | 6.7 |
| **11d** | | OH | Me | H | H | H | NS | NT | NT |
| **12a** |  | OH | H | H | H | H | NA | NT | 0 |
| **12b** | | OH | H | H | Cl | H | NA | NT | 0 |
| **12c** | | OH | H | OMe | H | H | NA | NT | 0 |
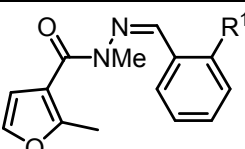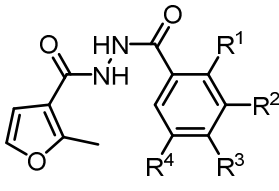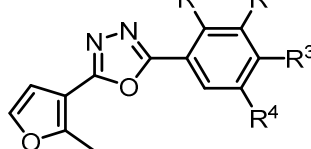
**Table 1**. Inhibition of *Sm*NACE and human CD38[b]

[a]*In vitro* assay. The given $IC_{50}$ values are the means of three independent determinations using the fluorimetric assay for compounds **3a**-**3e**; [b]NS = Not soluble; NA = Not active (0% inhibition at 100 µM); PI = Percent of inhibition of human CD38 at 100 µM as measured using the HPLC assay; NT = Not tested (PI were not determined if $IC_{50(Sm\text{NACE})}$ > 100 µM or if $IC_{50(hCD38)}$ were determined, $IC_{50}$ were not determined if no inhibition was observed at 100 µM). [c]The Z-isomeric form of hydrazone was suggested by docking studies (Figure S1).

AUTHOR INFORMATION

**Corresponding Authors**

* E-mail: ekellen@unistra.fr. Phone: (+33)368854221. Fax: (+33)368854310.

* E-mail: steffner@unistra.fr. Phone: (+33) 368854169. Fax: (+33)368854306.

**Author Contributions**

SAJ conceived, designed and performed experiments, analyzed and interpreted data, and contributed to the writing of the manuscript. IK and OK performed experiments and analyzed data. FS, FEL and AW contributed to the study design and provided support. HMS and EK designed the study, analyzed and interpreted data and wrote the manuscript.

ABBREVIATIONS

*Sm*NACE, *Schistosoma mansoni* $NAD^+$ catabolizing enzyme; $\varepsilon$-$NAD^+$, $1,N^6$-etheno $NAD^+$ .

REFERENCES

1.  Colley, D. G.; Bustinduy, A. L.; Secor, W. E.; King, C. H. Human schistosomiasis. *Lancet* **2014,** 383, 2253-2264.

2.  World Health Organization. Schistosomiasis. Fact sheet N°115. http://www.who.int/mediacentre/factsheets/fs115 (01/06/2015).

3.  Pearce, E. J.; MacDonald, A. S. The immunobiology of schistosomiasis. *Nat. Rev. Immunol.* **2002,** 2, 499-511.

4.  Fairfax, K.; Nascimento, M.; Huang, S. C.-C.; Everts, B.; Pearce, E. J. Th2 responses in schistosomiasis. *Semin. Immunopathol.* **2012,** 34, 863-871.

5.  Hotez, P. J.; Bethony, J. M.; Diemert, D. J.; Pearson, M.; Loukas, A. Developing vaccines to combat hookworm infection and intestinal schistosomiasis. *Nat. Rev. Microbiol.* **2010,** 8, 814-826.

6.  Panic, G.; Duthaler, U.; Speich, B.; Keiser, J. Repurposing drugs for the treatment and control of helminth infections. *Int. J. Parasitol. Drugs Drug Resist.* **2014,** 4, 185-200.

7.  Goodrich, S. P.; Muller-Steffner, H.; Osman, A.; Moutin, M.-J.; Kusser, K.; Roberts, A.; Woodland, D. L.; Randall, T. D.; Kellenberger, E.; LoVerde, P. T.; Schuber, F.; Lund, F. E. Production of calcium-mobilizing metabolites by a novel member of the ADP-ribosyl cyclase family expressed in *Schistosoma mansoni*. *Biochemistry* **2005,** 44, 11082-11097.

8.  Partida-Sanchez, S.; Rivero-Nava, L.; Shi, G.; Lund, F. E. CD38: an ecto-enzyme at the crossroads of innate and adaptive immune responses. *Adv. Exp. Med. Biol.* **2007,** 590, 171-183.

9. Kuhn, I.; Kellenberger, E.; Rognan, D.; Lund, F. E.; Muller-Steffner, H.; Schuber, F. Redesign of *Schistosoma mansoni* NAD$^+$ catabolizing enzyme: active site H103W mutation restores ADP-ribosyl cyclase activity. *Biochemistry* **2006,** 45, 11867-11878.

10. Kuhn, I.; Kellenberger, E.; Said-Hassane, F.; Villa, P.; Rognan, D.; Lobstein, A.; Haiech, J.; Hibert, M.; Schuber, F.; Muller-Steffner, H. Identification by high-throughput screening of inhibitors of *Schistosoma mansoni* NAD(+) catabolizing enzyme. *Bioorg. Med. Chem.* **2010,** 18, 7900-7910.

11. Hopkins, A. L.; Groom, C. R.; Alex, A. Ligand efficiency: a useful metric for lead selection. *Drug Discov. Today* **2004,** 9, 430-431. In the present article, the ligand efficiency formula is LE $= \dfrac{-1.363 \log \text{IC}_{50}}{\text{number of heavy atoms}}$

12. Shehata, I. A. Synthesis and antifungal activity of some new 1,2,4-triazole and furan containing compounds. *Saudi Pharm. J.* **2003,** 11, 87-96.

13. Shaber, S. H.; Webster, J. D.; Young, D. H. (Dow AgroSciences LLC) Synergistic fungicidal and algicidal compositions including 2-hydroxyphenylaldehyde and 2-hydroxyphenylketone heterocycloylhydrazones and copper. Eur. Pat. 2605653 A1, 2013.

14. Wu, P.-L.; Peng, S.-Y.; Magrath, J. 1-Acyl-2-alkylhydrazines by the reduction of acylhydrazones. *Synthesis* **1995**, 435–438.

15. Trahanovsky, W. S.; Huang, Y. J.; Leung, M. Effects of .alpha.-tert-butyl group substitution on the reactivity and dimerization products of furan-based o-quinodimethanes. *J. Org. Chem.* **1994,** 59, 2594-2598.

16.    Hansen, H. C.; Chiacchia, F. S.; Patel, R.; Wong, N. C. W.; Khlebnikov, V.; Jankowska, R.; Patel, K.; Reddy, M. M. Stilbene analogs as inducers of apolipoprotein-I transcription. *Eur. J. Med. Chem.* **2010,** 45, 2018-2023.

17.    Isobe, T.; Ishikawa, T. 2-Chloro-1,3-dimethylimidazolinium Chloride. 2. Its Application to the Construction of Heterocycles through Dehydration Reactions. *J. Org. Chem.* **1999,** 64, 6989-6992.

18.    Marcou, G.; Rognan, D. Optimizing fragment and scaffold docking by use of molecular interaction fingerprints. *J. Chem. Inf. Model.* **2007,** 47, 195-207.

19.    Muller, H. M.; Muller, C. D.; Schuber, F. NAD+ glycohydrolase, an ecto-enzyme of calf spleen cells. *Biochem. J.* **1983,** 212, 459-464.

Table of Contents Graphic



virtual screening

$IC_{50(SmNACE)} = 88\mu M$

$IC_{50(hCD38)} = 109\mu M$

SAR

$IC_{50(SmNACE)} = 33nM$

$IC_{50(hCD38)} > 100\mu M$